





Tryptophan extends the life of cytochrome P450

Raheleh Ravanfar^{a,1}, Yuling Sheng^a, Harry B. Gray^{a,2} , and Jay R. Winkler^{a,2} 

Contributed by Harry B. Gray; received October 6, 2023; accepted November 4, 2023; reviewed by Michael T. Green and Stephen G. Sligar

Powerfully oxidizing enzymes need protective mechanisms to prevent self-destruction. The flavocytochrome P450 BM3 from *Priestia megaterium* (P450_{BM3}) is a self-sufficient monooxygenase that hydroxylates fatty acid substrates using O₂ and NADPH as co-substrates. Hydroxylation of long-chain fatty acids ($\geq C_{14}$) is well coupled to O₂ and NADPH consumption, but shorter chains ($\leq C_{12}$) are more poorly coupled. Hydroxylation of *p*-nitrophenoxydodecanoic acid by P450_{BM3} produces a spectrophotometrically detectable product wherein the coupling of NADPH consumption to product formation is just 10%. Moreover, the rate of NADPH consumption is 1.8 times that of O₂ consumption, indicating that an oxidase uncoupling pathway is operative. Measurements of the total number of enzyme turnovers before inactivation (TTN) indicate that higher NADPH concentrations increase TTN. At lower NADPH levels, added ascorbate increases TTN, while a W96H mutation leads to a decrease. The W96 residue is about 7 Å from the P450_{BM3} heme and serves as a gateway residue in a tryptophan/tyrosine (W/Y) hole transport chain from the heme to a surface tyrosine residue. The data indicate that two oxidase pathways protect the enzyme from damage by intercepting the powerfully oxidizing enzyme intermediate (Compound I) and returning it to its resting state. At high NADPH concentrations, reducing equivalents from the flavoprotein are delivered to Compound I by the usual reductase pathway. When NADPH is not abundant, however, oxidizing equivalents from Compound I can traverse a W/Y chain, arriving at the enzyme surface where they are scavenged by reductants. Ubiquitous tryptophan/tyrosine chains in highly oxidizing enzymes likely perform similar protective functions.

cytochrome P450 | tryptophan | tyrosine | total turnover number | protection

The oxygenation of Earth's atmosphere by cyanobacteria some 2.4 billion years ago provided a powerful and highly reactive energy source for living organisms (1). This toxic atmospheric pollutant was likely fatal to many anaerobic organisms that had evolved in the prior anoxic environment. The evolutionary challenge was to exploit the power of this new oxidant while mitigating deleterious side effects (2, 3). Prime examples of adaptation to the oxygen atmosphere are the cytochromes P450 (P450). These heme-thiolate proteins are members of a superfamily of enzymes that consume NAD(P)H to catalyze the incorporation of one oxygen atom from O₂ into an organic substrate, with the second oxygen atom released in a water molecule (4). The oldest P450s from the CYP51 family are involved in steroid synthesis (5) and are thought to have arisen early in the oxygenation of the atmosphere (6, 7). Today, more than 2,000 CYP families (enzymes within a family have >40% sequence identity) among all branches of life (8, 9) perform an extraordinarily diverse array of biological functions (10).

The canonical P450 catalytic mechanism involves no fewer than 6 carefully choreographed steps, including substrate binding and delivery of reducing equivalents (Fig. 1) (4). The key intermediate in catalysis is Compound I (CI) (11), a ferryl-porphyrin radical (Fe^{IV}(O)P[•]) that abstracts a hydrogen atom from the substrate (RH), producing Fe^{IV}(OH)P (Compound II, CII) and a substrate radical (R[•]). Hydroxyl rebound to R[•] forms the product (ROH) and regenerates the resting ferric enzyme.

In the exhaustively studied bacterial enzyme from *Pseudomonas putida* (CYP101A1), *d*-camphor is hydroxylated with nearly perfect regio- and stereoselectivity, consuming one molecule each of NADPH and O₂ and producing *d*-5-*exo*-hydroxycamphor and water (12). When an alternative substrate is used (e.g., norcamphor), however, selectivity is degraded and the tight stoichiometric coupling between NADPH and O₂ consumption in relation to product formation is compromised (12–14). Indeed, subsequent studies have demonstrated that uncoupled catalysis is a common feature in many P450s (15). Three uncoupling pathways (shunts) identified in the P450 cycle (Fig. 1) produce superoxide, hydrogen peroxide, or water instead of hydroxylated substrate. We have suggested that electron transport chains in P450 composed of tryptophan (W) and tyrosine (Y) residues participate in the water-producing oxidase shunt to protect the enzyme from damage when substrate hydroxylation is impaired (16–21).

Significance

Many enzymes that utilize oxygen and hydrogen peroxide generate powerfully oxidizing reactive intermediates that have the potential to damage the protein scaffold when reaction with substrate fails. A longstanding question about these enzymes is how they avoid self-destruction during catalysis. The cytochrome P450 monooxygenase from *Priestia megaterium* solves this problem by deactivating the reactive intermediate using electron transfer along a chain of tryptophan and tyrosine residues. When this chain is disrupted, the enzyme completes many fewer catalytic cycles before it is deactivated. Redox-active tryptophan/tyrosine chains could provide a general means of extending the functional lifetimes of oxidizing enzymes.

Author affiliations: ^aBeckman Institute, California Institute of Technology, Pasadena, CA 91125

Author contributions: H.B.G. and J.R.W. designed research; R.R. and Y.S. performed research; R.R., H.B.G., and J.R.W. analyzed data; and R.R., H.B.G., and J.R.W. wrote the paper.

Reviewers: M.T.G., University of California, Irvine; and S.G.S., University of Illinois Urbana-Champaign.

The authors declare no competing interest.

Copyright © 2023 the Author(s). Published by PNAS. This article is distributed under [Creative Commons Attribution-NonCommercial-NoDerivatives License 4.0 \(CC BY-NC-ND\)](https://creativecommons.org/licenses/by-nc-nd/4.0/).

¹Present address: Department of Chemistry and Biochemistry, Texas Tech University, Lubbock, TX 79409.

²To whom correspondence may be addressed. Email: hbgray@caltech.edu or winklerj@caltech.edu.

This article contains supporting information online at <https://www.pnas.org/lookup/suppl/doi:10.1073/pnas.2317372120/-DCSupplemental>.

Published December 7, 2023.

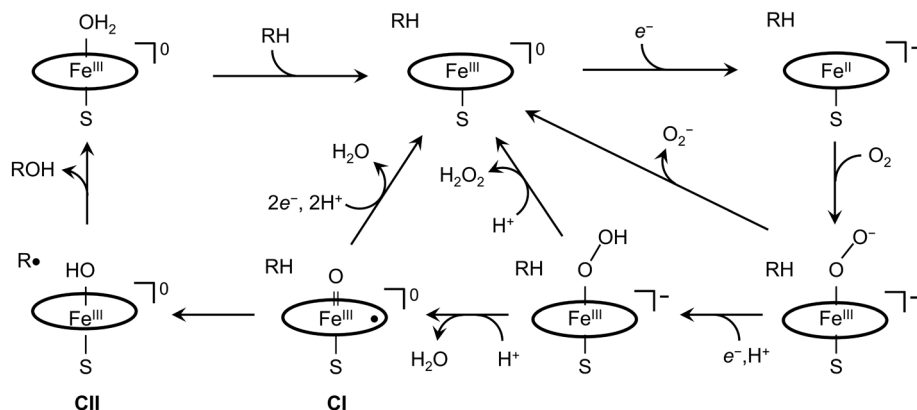


Fig. 1. Reaction pathways in cytochrome P450 catalysis. The peripheral pathway involves productive substrate (RH) hydroxylation using reducing equivalents (e^-) sourced from NAD(P)H through a reductase. The three shunt pathways intercept intermediates producing superoxide, hydrogen peroxide, or water.

We chose cytochrome P450_{BM3} from *Bacillus megaterium* (now *Priestia megaterium*) (CYP102A1) to explore whether W/Y chains protect the enzyme from damage during catalysis. P450_{BM3} is a self-sufficient hydroxylase comprised of heme and reductase domains fused in a single polypeptide (22). Interestingly, sequence alignments and structural analyses indicate that both P450_{BM3} domains are more closely related to eukaryotic microsomal analogues than to prokaryotic enzymes (23–25). Catalysis is initiated by the addition of the substrate and NADPH to an enzyme solution in aerated buffer. Although the natural P450_{BM3} substrate is not known with certainty, the enzyme efficiently catalyzes hydroxylation of long-chain fatty acids at the ω -1, ω -2, and ω -3 positions (26). Analysis of the P450_{BM3} heme domain (27) revealed a potential electron-transport (ETr) chain comprised of W96/W90/Y334 provides a conduit for oxidizing equivalents (holes) to escape from the heme and migrate to the enzyme surface (Fig. 2) where they can be scavenged by cellular reductants (20). Using a spectroscopic probe of P450_{BM3} catalysis, we have examined the survival of the wild-type enzyme and several mutants to explore the potential protective role of this ETr chain.

Results

The substrate in our investigations of P450_{BM3} catalysis is *p*-nitrophenoxydodecanoic acid (12-*p*NCA) (28). Hydroxylation of 12-*p*NCA at the ω -1 position produces an unstable hemiacetal that

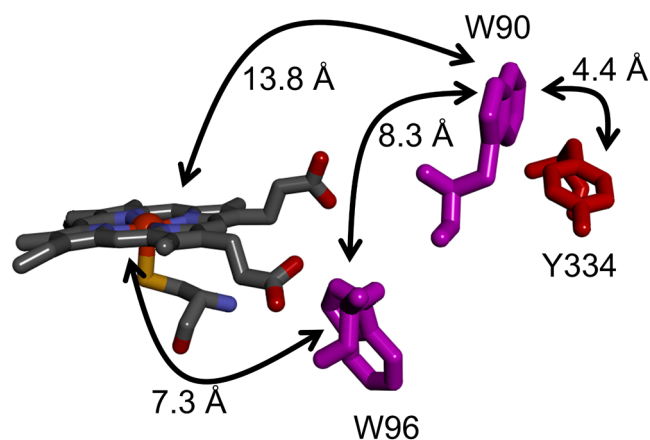


Fig. 2. Structural model of the W/Y electron transport chain in P450_{BM3} extending from the heme to the surface exposed Y334 residue. Electron transfer distances are taken from PDB ID 2Jl2, ref. 21. Sidechain solvent accessibilities are W96, 0.5%; W90, 34%; Y334, 32% (SI Appendix).

releases a spectrophotometrically detectable product, *p*-nitrophenolate. In prior work, we examined 12-*p*NCA oxidation kinetics and coupling efficiency catalyzed by wild-type (WT) P450_{BM3} and 3 mutant enzymes (W96H, W96H|W90F, W96H|W90F|Y334F). The activities of the mutant enzymes, defined by the ratio of Michaelis–Menten parameters k_{cat}/K_M , differed from that of WT by less than 50%. The coupling efficiency, defined as the yield of hydroxylated product divided by NADPH consumed, was $(10 \pm 2)\%$ for all four enzymes. Overall, mutation of the residues in the ETr chain had very little impact on P450_{BM3} kinetics or product yield.

The superoxide and peroxide shunt pathways (Fig. 1) seemed the likely avenues for P450_{BM3} uncoupling with the 12-*p*NCA substrate. Analysis of H₂O₂ produced during enzyme turnover, however, revealed that it amounted to less than 10% of the NADPH consumed, indicating a minor uncoupling role for the superoxide and peroxide shunts. By elimination, then, the oxidase shunt in which two electrons and two protons are delivered to **CI** likely accounts for most of the uncoupling in P450_{BM3} catalyzed 12-*p*NCA oxidation. A critical distinction between the oxidase shunt and the superoxide and peroxide shunts is the ratio of NADPH to O₂ consumption: 2:1 for the oxidase pathway and 1:1 for superoxide and peroxide. We measured rates of O₂ and NADPH consumption during catalysis of 12-*p*NCA oxidation by P450_{BM3} and found a ratio of 1.8, confirming a dominant role for the oxidase uncoupling pathway.

If uncoupled turnover through the oxidase shunt pathway protects the enzyme from damage in the event of impaired substrate oxidation, then its effectiveness should be apparent in the total number of turnovers (TTN) the enzyme performs before it is inactivated. In our prior investigation, we found that TTN values in W96H, W96H|W90F, and W96H|W90F|Y334 mutants were 50 to 70% of WT values (21). We have found that TTNs for P450_{BM3} catalyzed oxidation of 12-*p*NCA are a sensitive function of the NADPH concentration. With 300 μ M NADPH, the enzyme catalyzes 635 ± 9 turnovers before inactivation. With 50 μ M NADPH, however, the enzyme is inactivated after just 132 ± 9 turnovers (Table 1 and Fig. 3). If the W96|W90|Y334 ETr pathway is active in protecting the enzyme by shuttling holes to the enzyme surface, then mutating the first residue in the pathway should negatively impact TTN. At high NADPH concentration, introduction of the W96H mutation has a relatively minor effect on TTN, decreasing to 84% of the WT value. As the NADPH concentration is lowered, however, the impact of the W96H mutation increases such that when [NADPH] = 50 μ M, TTN of the mutant is just 54% of that for WT.

The oxidase shunt pathway requires reducing equivalents to convert **CI** back to the resting ferric state of the enzyme. We explored

Table 1. Total turnover numbers (TTN) for WT and W96H catalyzed oxidation of 12-*p*NCA

Enzyme	[NADPH] / μ M ([Asc] = 0)			[NADPH] / μ M ([Asc] = 100 μ M)	
	50	100	300	50	300
WT P450 _{BM3}	132 \pm 5	344 \pm 20*	635 \pm 9	245 \pm 24	618 \pm 19
W96H P450 _{BM3}	71 \pm 4	225 \pm 3*	534 \pm 7	87 \pm 9	562 \pm 24

*Ref. 21.

the effect on TTN of added ascorbate (100 μ M) for WT and W96H P450_{BM3}. At high NADPH concentration, ascorbate has little impact on TTN for both WT and W96H enzymes. At low NADPH concentration, however, ascorbate nearly doubles TTN in the WT enzyme. This result contrasts with that of the W96H mutant where 100 μ M ascorbate produces only a modest increase in TTN.

Discussion

Although the natural substrate for P450_{BM3} has not been identified definitively, the coupling efficiencies for hydroxylation of straight-chain fatty acids range from 34 \pm 7% for lauric acid to 93 \pm 3% for palmitic acid (29, 30). These coupling efficiencies parallel the dissociation constants of the acids (lauric acid, 43 μ M; palmitic acid, 0.1 μ M). The coupling efficiency for the 12-*p*NCA substrate is just 12%, indicating that introduction of the aromatic group at the end of the 12-carbon fatty acid further disrupts substrate binding. The ratio of NADPH to O₂ consumption rates (1.8) strongly indicates that most of the uncoupling with 12-*p*NCA proceeds through the oxidase shunt.

The dependence of TTN on NADPH concentration implicates the natural electron transfer (ET) route from the reductase domain to the heme domain in the oxidase shunt pathway. The P450_{BM3} enzyme is an unusual homodimer in which the reductase domain of one monomer delivers electrons to the heme domain of the other (31, 32). This redox model contrasts with that of the more common P450s that obtain reducing equivalents from one or more separate redox partners (33). For these enzymes, low-driving-force interprotein ET is typically rate limiting in catalysis (34, 35). Elimination of the bimolecular step in P450_{BM3} produces relatively rapid delivery of reducing equivalents ($k > 10^7$ s⁻¹) (25, 36, 37), making this enzyme among the fastest in the P450 superfamily. That the W96H mutation has little impact on enzyme survival at high NADPH concentration reflects the efficiency of electron

delivery from the reductase domain. When the NADPH concentration is lowered to 50 μ M, electron delivery from the reductase domain slows and TTN decreases. Under these conditions, the W96 residue is much more important for enzyme survival. When the NADPH concentration is low, addition of ascorbate produces a substantial increase in TTN for the WT enzyme but has little effect on the W96H mutant. These observations are consistent with a second oxidase shunt pathway involving the W96|W90|Y334 ETr chain.

We suggest that when **CI** fails to abstract a hydrogen atom from the substrate, W96 reduces the porphyrin radical, and the hole further migrates via W90 to the enzyme surface, forming a Y334 radical. NADPH is a two-electron reductant and likely could not readily reduce a tyrosine radical. Ascorbate, on the other hand, can reduce the tyrosine radical and protect the enzyme from damage. The W96H mutation disrupts this ETr pathway so that addition of ascorbate during enzyme catalysis does not substantially improve TTN. W96 appears to be the critical residue in the second oxidase shunt pathway. It is a highly conserved residue in CYP102, appearing in all but one of 250 sequences (*SI Appendix*). It is noteworthy that in bacterial P450 enzymes, a histidine residue appears more commonly at this location. In eukaryotes, however, tryptophan typically occupies this site (38). The other two sites in the putative W96|W90|Y334 ETr pathway are far less well conserved (W90, 20%; Y334 65%), implying that multiple hole migration routes to the surface might be available.

Concluding Remarks

Uncoupled substrate hydroxylation has been characterized in many cytochromes P450, and the oxidase shunt pathway frequently is involved (12, 13, 39–42). Our TTN determinations demonstrate that the oxidase shunt protects P450_{BM3} from inactivation during catalysis. Two oxidase pathways appear to operate in P450_{BM3}. The first pathway exploits ET from the reductase domain to the heme. The uncommon fusion of reductase and heme domains in P450_{BM3} renders this intraprotein ET pathway particularly effective when the NADPH concentration is high. At low NADPH concentrations, a second protective pathway utilizing W96 becomes important. The biological significance of the two pathways depends on the intracellular concentration of NADPH in *Priestia megaterium*. Estimates of intracellular NADPH concentrations in bacterial cells fall in the 20- to 300- μ M range (43–47). A similarly wide variation has been reported for eukaryotic cells (48–51). This broad concentration range depends on growth conditions, cell type, and analytical method and spans the regions of dominance for the two pathways. When NADPH is abundant, protection can be afforded by the reductase. When NADPH is scarce, the W96 pathway can protect P450_{BM3} by extracting reducing equivalents from the high intracellular concentration of glutathione (43) and delivering them to **CI** and **CII** before either highly oxidizing intermediate can damage the enzyme.

The fusion of reductase and oxidase domains into a single polypeptide in P450_{BM3} is rare. The usual delivery of electrons to cytochromes P450 involves reaction with a separate reductase. Bimolecular reduction of **CI** and **CII** by an enzyme diffusing in the cytoplasm or in a lipid membrane will be much less efficient than the intraprotein electron delivery in P450_{BM3}. In cytochromes P450 lacking a fused reductase domain, W/Y hole transport pathways likely will assume a greater role in protecting the enzyme from damage during catalysis.

Our studies provide evidence that a hole transport pathway through W96 can extend the functional lifetime of P450_{BM3}. A single protection event can, in principle, double the functional lifetime of an enzyme. The data, however, do not tell us whether the

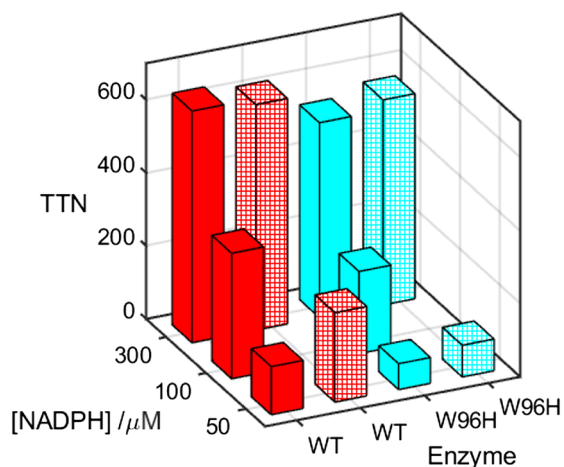


Fig. 3. Total turnover numbers (TTN) for WT (red) and W96H (cyan) P450_{BM3} catalyzed aerobic oxidation of 12-*p*NCA (25 μ M) at three NADPH concentrations in the absence (solid bars) and presence of 100 μ M ascorbate (patterned bars).

W96 pathway is an evolutionary adaptation in *Priestia megaterium* or simply an in vitro curiosity. Recent studies have indicated that high enzyme replacement rates reduce an organism's productivity (52). Detailed analysis of *Lactococcus lactis* growth revealed that protein synthesis and turnover consume at least half of cellular ATP (53). Comparison of two *Saccharomyces cerevisiae* strains demonstrated that biomass yields were lower in the strain with greater protein turnover (54, 55). The energetic burden that high protein turnover imposes on a cell suggests that protective mechanisms that extend enzyme lifetime provide a selective advantage to an organism. Many other oxidizing enzymes have highly reactive intermediates that potentially endanger their viability. Our analysis of protein structures found that W/Y chains are common in enzymes that utilize O₂ as a substrate (16, 20). Results with P450_{BM3} support the hypothesis (16–20) that redox-active W/Y chains extend the functional lifetimes of oxidizing enzymes.

Materials and Methods

Wild-type and mutant proteins used in this study were prepared by heterologous expression in *E. coli* using standard procedures that have been described previously (21) and are described in further detail in *SI Appendix*. The amino acid and nucleotide sequences for wild-type P450_{BM3}, as well as the primers used

for site-directed mutants, are listed in *SI Appendix*. All proteins were purified by ion-exchange chromatography.

Total turnover numbers were evaluated spectroscopically by quantifying the total amount of *p*-nitrophenolate produced by P450_{BM3} with the 12-*p*NCA substrate. Reaction products were periodically separated from the enzyme by ultrafiltration. Reactions were continued until catalysis ceased (*SI Appendix*). Kinetics of O₂ consumption were measured using a NeoFox optical oxygen sensing system (Ocean Optics, Largo, FL). NADPH consumption kinetics were measured spectrophotometrically. Hydrogen peroxide produced in P450_{BM3} catalysis was determined using an Abcam (Cambridge, UK) peroxide assay kit (ab272537). Calibration details are provided in *SI Appendix*.

Additional experimental details are provided in *SI Appendix*.

Data, Materials, and Software Availability. All study data are included in the article and/or supporting information.

ACKNOWLEDGMENTS. We thank Maryann Morales and Jill Clinton for invaluable laboratory assistance and many helpful discussions during this research. Research reported in this publication was supported by the National Institute of Diabetes and Digestive and Kidney Diseases of the NIH under award number R01DK019038 (H.B.G. and J.R.W.). The content is solely the responsibility of the authors and does not necessarily represent the official views of the NIH. Additional support for this work was provided by the Arnold and Mabel Beckman Foundation (H.B.G. and J.R.W.).

1. J. Olejarz, Y. Iwasa, A. H. Knoll, M. A. Nowak, The Great Oxygenation Event as a consequence of ecological dynamics modulated by planetary change. *Nat. Commun.* **12**, 3985 (2021), 10.1038/s41467-021-23286-7.
2. W. W. Fischer, J. Hemp, J. S. Valentine, How did life survive Earth's great oxygenation? *Curr. Opin. Chem. Biol.* **31**, 166–178 (2016), 10.1016/j.cbpa.2016.03.013.
3. J. P. Klinman, How do enzymes activate oxygen without inactivating themselves? *Acc. Chem. Res.* **40**, 325–333 (2007), 10.1021/ar6000507.
4. I. G. Denisov, T. M. Makris, S. G. Sligar, I. Schlichting, Structure and chemistry of cytochrome P450. *Chem. Rev.* **105**, 2253–2277 (2005), 10.1021/cr0307143.
5. Y. Yoshida *et al.*, Structural and evolutionary studies on sterol 14-demethylase P450 (CYP51), the most conserved P450 monooxygenase: II. Evolutionary analysis of protein and gene structures. *J. Biochem.* **122**, 1122–1128 (1997), 10.1093/oxfordjournals.jbchem.a021870.
6. B. Rasmussen, I. R. Fletcher, J. J. Brocks, M. R. Kilburn, Reassessing the first appearance of eukaryotes and cyanobacteria. *Nature* **455**, 1101–1104 (2008), 10.1038/nature07381.
7. J. R. Waldbauer, D. K. Newman, R. E. Summons, Microaerobic steroid biosynthesis and the molecular fossil record of Archean life. *Proc. Natl. Acad. Sci. U.S.A.* **108**, 13409–13414 (2011), 10.1073/pnas.1104160108.
8. D. R. Nelson, Cytochrome P450 diversity in the tree of life. *Biochim. Biophys. Acta Proteins Proteom.* **1866**, 141–154 (2018), 10.1016/j.bbapap.2017.05.003.
9. M. Parvez *et al.*, Molecular evolutionary dynamics of cytochrome P450 monooxygenases across kingdoms: Special focus on mycobacterial P450s. *Sci. Rep.* **6**, 33099 (2016), 10.1038/srep33099.
10. D. Werck-Reichhart, R. Feyereisen, Cytochromes P450: A success story. *Gen. Biol.* **1**, REVIEWS3003 (2000), 10.1186/gb-2000-1-6-reviews3003.
11. J. Rittle, M. T. Green, Cytochrome P450 compound I: Capture, characterization, and C–H bond activation kinetics. *Science* **330**, 933–937 (2010), 10.1126/science.1193478.
12. W. M. Atkins, S. G. Sligar, Metabolic switching in cytochrome P-450_{am}: Deuterium isotope effects on regioselectivity and the monooxygenase/oxidase ratio. *J. Am. Chem. Soc.* **109**, 3754–3760 (1987), 10.1021/ja00246a038.
13. W. M. Atkins, S. G. Sligar, Deuterium isotope effects in norcamphor metabolism by cytochrome P-450_{am}: Kinetic evidence for the two-electron reduction of a high-valent iron-oxo intermediate. *Biochemistry* **27**, 1610–1616 (1988), 10.1021/bi00405a033.
14. S. Kadhodayan, E. D. Coulter, D. M. Maryniak, T. A. Bryson, J. H. Dawson, Uncoupling oxygen transfer and electron transfer in the oxygenation of camphor analogues by cytochrome P450-CAM: Direct observation of an intermolecular isotope effect for substrate C–H activation. *J. Biol. Chem.* **270**, 28042–28048 (1995), 10.1074/jbc.270.47.28042.
15. Y. V. Grinkova, I. G. Denisov, M. A. McLean, S. G. Sligar, Oxidase uncoupling in heme monooxygenases: Human cytochrome P450 CYP3A4 in Nanodiscs. *Biochem. Biophys. Res. Commun.* **430**, 1223–1227 (2013), 10.1016/j.bbrc.2012.12.072.
16. H. B. Gray, J. R. Winkler, Hole hopping through tyrosine/tryptophan chains protects proteins from oxidative damage. *Proc. Natl. Acad. Sci. U.S.A.* **112**, 10920–10925 (2015), 10.1073/pnas.1512704112.
17. J. R. Winkler, H. B. Gray, Electron flow through biological molecules: Does hole hopping protect proteins from oxidative damage? *Quart. Rev. Biophys.* **48**, 411–420 (2015), 10.1017/s0033583515000062.
18. H. B. Gray, J. R. Winkler, The rise of radicals in bioinorganic chemistry. *Isr. J. Chem.* **56**, 640–648 (2016), 10.1002/ijch.201600069.
19. H. B. Gray, J. R. Winkler, Living with oxygen. *Acc. Chem. Res.* **51**, 1850–1857 (2018), 10.1021/acs.accounts.8b00245.
20. H. B. Gray, J. R. Winkler, Functional and protective hole hopping in metalloenzymes. *Chem. Sci.* **12**, 13988–14003 (2021), 10.1039/D1SC04286F.
21. R. Ravanfar, Y. Sheng, H. B. Gray, J. R. Winkler, Tryptophan-96 in cytochrome P450 BM3 plays a key role in enzyme survival. *FEBS Lett.* **597**, 59–64 (2023), 10.1002/1873-3468.14514.
22. L. O. Narhi, A. J. Fulco, Characterization of a catalytically self-sufficient 119,000-dalton cytochrome P-450 monooxygenase induced by barbiturates in *Bacillus megaterium*. *J. Biol. Chem.* **261**, 7160–7169 (1986).
23. T. D. Porter, An unusual yet strongly conserved flavoprotein reductase in bacteria and mammals. *Trends Biochem. Sci.* **16**, 154–158 (1991), 10.1016/0968-0004(91)90059-5.
24. D. F. V. Lewis, E. Watson, B. G. Lake, Evolution of the cytochrome P450 superfamily: Sequence alignments and pharmacogenetics. *Mutat. Res.* **410**, 245–270 (1998), 10.1016/S1383-5742(97)00040-9.
25. C. J. C. Whitehouse, S. G. Bell, L. L. Wong, P450_{BM3} (CYP102A1): Connecting the dots. *Chem. Soc. Rev.* **41**, 1218–1260 (2012), 10.1039/c1cs15192d.
26. Y. Miura, A. J. Fulco, ω -1, ω -2 and ω -3 Hydroxylation of long-chain fatty acids, amides and alcohols by a soluble enzyme system from *Bacillus megaterium*. *Biochim. Biophys. Acta Lipids Lipid Metab.* **388**, 305–317 (1975), 10.1016/0005-2760(75)90089-2.
27. H. M. Girvan *et al.*, Structural and spectroscopic characterization of P450 BM3 mutants with unprecedented P450 heme iron ligand sets - New heme ligation states influence conformational equilibria in P450 BM3. *J. Biol. Chem.* **282**, 564–572 (2007), 10.1074/jbc.M607949200.
28. U. Schwaneberg, C. Schmidt-Dannert, J. Schmitt, R. D. Schmid, A Continuous spectrophotometric assay for P450 BM-3, a fatty acid hydroxylating enzyme, and its mutant F87A. *Anal. Biochem.* **269**, 359–366 (1999), 10.1006/abio.1999.4047.
29. M. J. Cryle, J. J. De Voss, Facile determination of the absolute stereochemistry of hydroxy fatty acids by GC: Application to the analysis of fatty acid oxidation by a P450BM3 mutant. *Tetrahedron* **18**, 547–551 (2007), 10.1016/j.tetasy.2007.01.034.
30. M. J. Cryle, J. J. De Voss, The role of the conserved threonine in P450BM3 oxygen activation: Substrate-determined hydroxylation activity of the Thr268Ala mutant. *ChemBioChem* **9**, 261–266 (2008), 10.1002/cbic.200700537.
31. H. Zhang *et al.*, The full-length cytochrome P450 enzyme CYP102A1 dimerizes at its reductase domains and has flexible heme domains for efficient catalysis. *J. Biol. Chem.* **293**, 7727–7736 (2018), 10.1074/jbc.RA117.000600.
32. M. Su, S. Chakraborty, Y. Osawa, H. Zhang, Cryo-EM reveals the architecture of the dimeric cytochrome P450 CYP102A1 enzyme and conformational changes required for redox partner recognition. *J. Biol. Chem.* **295**, 1637–1645 (2020), 10.1074/jbc.RA119.011305.
33. D. J. Cook, J. D. Finnigan, K. Cook, G. W. Black, S. J. Charnock, "Chapter Five—Cytochromes P450: History, classes, catalytic mechanism, and industrial application" in *Advances in Protein Chemistry and Structural Biology*, C. Z. Christov, Ed. (Academic Press, 2016), vol. 105, pp. 105–126.
34. M. M. Purdy, L. S. Koo, P. R. Ortiz de Montellano, J. P. Klinman, Steady-state kinetic investigation of cytochrome P450cam: Interaction with redox partners and reaction with molecular oxygen. *Biochemistry* **43**, 271–281 (2004), 10.1021/bi0356045.
35. M. M. Purdy, L. S. Koo, P. R. Ortiz de Montellano, J. P. Klinman, Mechanism of O₂ activation by cytochrome P450cam studied by isotope effects and transient state kinetics. *Biochemistry* **45**, 15793–15806 (2006), 10.1021/bi061726w.
36. I. Sevriukova, C. Shaffer, D. P. Ballou, J. A. Peterson, Equilibrium and transient state spectrophotometric studies of the mechanism of reduction of the flavoprotein domain of P450BM-3. *Biochemistry* **35**, 7058–7068 (1996), 10.1021/bi960060a.
37. J. T. Hazzard, S. Govindaraj, T. L. Poulos, G. Tollin, Electron transfer between the FMN and heme domains of cytochrome P450BM-3: Effects of substrate and CO. *J. Biol. Chem.* **272**, 7922–7926 (1997), 10.1074/jbc.272.12.7922.
38. M. L. H. Sørensen *et al.*, Hole hopping through cytochrome P450. *J. Phys. Chem. B* **124**, 3065–3073 (2020), 10.1021/acs.jpcc.9b09414.
39. F. De Matteis, D. P. Ballou, M. J. Coon, R. W. Estabrook, D. C. Haines, Peroxidase-like activity of uncoupled cytochrome P450 Studies with bilirubin and toxicological implications of uncoupling. *Biochem. Pharmacol.* **84**, 374–382 (2012), 10.1016/j.bcp.2012.04.016.
40. P. J. Loida, S. G. Sligar, Molecular recognition in cytochrome P-450: Mechanism for the control of uncoupling reactions. *Biochemistry* **32**, 11530–11538 (1993), 10.1021/bi00094a009.

41. H. Yeom, S. G. Sligar, Oxygen activation by cytochrome P450_{BM3}: Effects of mutating an active site acidic residue. *Arch. Biochem. Biophys.* **337**, 209–216 (1997), 10.1006/abbi.1996.9763.
42. D. Pompon, Rabbit liver cytochrome P-450 LM₂: Roles of substrates, inhibitors, and cytochrome b₅ in modulating the partition between productive and abortive mechanisms. *Biochemistry* **26**, 6429–6435 (1987), 10.1021/bi00394a020.
43. B. D. Bennett *et al.*, Absolute metabolite concentrations and implied enzyme active site occupancy in *Escherichia coli*. *Nat. Chem. Biol.* **5**, 593–599 (2009), 10.1038/nchembio.186.
44. L. García-Calvo *et al.*, Central carbon metabolite profiling reveals vector-associated differences in the recombinant protein production host *Escherichia coli* BL21. *Front. Chem. Engineering* **5**, (2023), 10.3389/fceng.2023.1142226.
45. L. M. Røst, A. Shafaei, K. Fuchino, P. Bruheim, Zwitterionic HILIC tandem mass spectrometry with isotope dilution for rapid, sensitive and robust quantification of pyridine nucleotides in biological extracts. *J. Chromatography B* **1144**, 122078 (2020), 10.1016/j.jchromb.2020.122078.
46. L. B. Thorfinnsdottir, L. García-Calvo, G. H. Bø, P. Bruheim, L. M. Røst, Optimized fast filtration-based sampling and extraction enables precise and absolute quantification of the *Escherichia coli* central carbon metabolome. *Metabolites* **13**, 150 (2023).
47. K. Tanaka *et al.*, Quantification of NAD(P)H in cyanobacterial cells by a phenol extraction method. *Photosynth. Res.* **148**, 57–66 (2021), 10.1007/s11120-021-00835-1.
48. K. Kumar, P. Bruheim, Large dependency of intracellular NAD and CoA pools on cultivation conditions in *Saccharomyces cerevisiae*. *BMC Res. Notes* **14**, 372 (2021), 10.1186/s13104-021-05783-6.
49. W. Lu, L. Wang, C. Li, S. Hui, J. D. Rabinowitz, Extraction and quantitation of nicotinamide adenine dinucleotide redox cofactors. *Antioxid. Redox Signal.* **28**, 167–179 (2018), 10.1089/ars.2017.7014.
50. R. M. Seifar *et al.*, Quantitative analysis of intracellular coenzymes in *Saccharomyces cerevisiae* using ion pair reversed phase ultra high performance liquid chromatography tandem mass spectrometry. *J. Chromatography A* **1311**, 115–120 (2013), 10.1016/j.chroma.2013.08.076.
51. R. Tao *et al.*, Genetically encoded fluorescent sensors reveal dynamic regulation of NADPH metabolism. *Nat. Methods* **14**, 720–728 (2017), 10.1038/nmeth.4306.
52. A. D. Hanson *et al.*, The number of catalytic cycles in an enzyme's lifetime and why it matters to metabolic engineering. *Proc. Natl. Acad. Sci. U.S.A.* **118**, e2023348118 (2021), 10.1073/pnas.2023348118.
53. P.-J. Lahtvee, A. Seiman, L. Arike, K. Adamberg, R. Vilu, Protein turnover forms one of the highest maintenance costs in *Lactococcus lactis*. *Microbiol.* **160**, 1501–1512 (2014), 10.1099/mic.0.078089-0.
54. K.-K. Hong, J. Hou, S. Shoaie, J. Nielsen, S. Bordel, Dynamic ¹³C-labeling experiments prove important differences in protein turnover rate between two *Saccharomyces cerevisiae* strains. *FEMS Yeast Res.* **12**, 741–747 (2012), 10.1111/j.1567-1364.2012.00823.x.
55. A. B. Canelas *et al.*, Integrated multilaboratory systems biology reveals differences in protein metabolism between two reference yeast strains. *Nat. Commun.* **1**, 145 (2010), 10.1038/ncomms1150.